# CONTROL-BASED CONTINUATION OF PERIODIC ORBITS WITH A TIME-DELAYED DIFFERENCE SCHEME

J. SIEBER & B. KRAUSKOPF

Department of Engineering Mathematics, University of Bristol,
Queen's Building, Bristol BS8 1TR, UK

June 5, 2006

## Abstract

This paper presents a method that is able to continue periodic orbits in systems where only output of the evolution over a given time period is available, which is the typical situation in an experiment. The starting point of our paper is an analysis of time-delayed feedback control, a method to stabilize periodic orbits experimentally that is popular among physicists. We show that the well-known topological limitations of this method can be overcome by an embedding into a pseudo-arclength continuation and prove that embedded time-delayed feedback control is able to stabilize periodic orbits that have at most one unstable Floquet multiplier sufficiently close to the unit circle. In the second part we introduce preconditioning into the time-delayed feedback control. In this way we extract a nonlinear system of equations from time profiles, which we solve using Newton iterations.

We demonstrate the feasibility of our method by continuing periodic orbits in a laser model through folds, and by computing the family of canard orbits of the classical stiff Van der Pol system with constant forcing.

# 1  Introduction

If a system under consideration is known in the form of a finite-dimensional system of ordinary differential equations (ODEs) then the continuation of stable and unstable stationary and time-periodic solutions and their bifurcations can be performed with existing numerical continuation software, for example, AUTO (Doedel *et al.* [1998]), or MatCont (Govaerts *et al.* [2000]; Dhooge *et al.* [2003]). The availability of these numerical tools for bifurcation analysis has been a breakthrough in the analysis of systems of ODEs of low dimension. Similar methods are emerging also for dynamical systems with an infinite-dimensional phase space but 'essentially low-dimensional' dynamics such as delay differential equations (Engelborghs *et al.* [2001]) or microscopic models (Kevrekidis *et al.* [2004]). One reason behind the success of numerical continuation tools is that they make phenomena (such as homoclinic cycles, or canard trajectories in singularly perturbed systems) visible that are notoriously difficult or even impossible to find in simulations and experiments, for example, due to their dynamical instability or their extreme sensitivity to perturbations.

The aim of this work is to make continuation techniques available also in an experimental setting. Our motivation comes from recent developments of the hybrid testing techniques known as *dynamic substructured testing*. The key idea of substructuring is to test a critical part of an engineering system in its original size in the laboratory under realistic loading conditions as if it were part of a bigger structure (Blakeborough *et al.* [2001]). To this end, the experiment is coupled to a computer simulation of the remainder of the system via sensors and actuators. While there are specific challenges to ensure its validity, hybrid testing holds great promise for the design and testing of future high-performance engineering systems. Dynamical systems techniques are now being introduced into substructured testing, especially for dealing with delay in the coupling between experiment and computer model (Wallace *et al.* [2005]; Kyrychko *et al.* [2005]).

The unique set-up of a hybrid test allows one to directly and easily change the parameters of the computer part of the test. In other words, this type of experiment is particularly amenable, at least in principle, to continuation techniques. However, as in any experiment, one needs to deal with a number of serious restrictions, namely

(R1) the absence of an overall model,

(R2) the impossibility to set initial conditions of the dynamical system, and

(R3) access to only a part of the state variables for measurement (output) or manipulation (input).

These restrictions rule out many of the proven approaches for the development of efficient and stable numerical algorithms.

In this paper we present two control-based methods for the continuation of periodic orbits that are not affected by the above restrictions. By way of a feasibility study for an experimental setting, the validity of our methods is demonstrated with numerical examples (under the restrictions (R1)–(R3)).

We start in Sec. 3 from time-delayed feedback control, introduced by Pyragas [1992, 2001] as a method for potential application in chaos control. This method solves a difference

equation simultaneous to the dynamical system with the aim of controlling to zero the difference between the current state and the state from one period ago. In Sec. 3 we summarize the known results on the applicability and limitations of time-delayed feedback control. We then prove that embedding this method into a continuation setting extends the scope of time-delayed feedback control considerably. The particular appeal of this approach is that it is known to be applicable to real experiments and does not require any approximate linearization of the flow. Our results guarantee that embedded time-delayed feedback control works in the vicinity of all codimension-one bifurcations that form stability boundaries of the system. We demonstrate this fact with a numerical study of periodic orbits in a laser model.

We then generalize the embedded time-delayed feedback control approach in Sec. 4 by presenting a way to extract a nonlinear system of equations from time profiles. If this infinite-dimensional system is solved by a Newton or Newton-Picard iteration (which requires an approximation of a linearization) then our approach corresponds to a preconditioned version of time-delayed feedback control. With this preconditioning the method is as robust as classical numerical methods but potentially applicable to experiments. We demonstrate the stability of these preconditioned iterations by computing the family of canard periodic orbits in the stiff Van der Pol oscillator with constant forcing — a classical example of a an extremely sensitive problem where simulations and methods based on single-shooting fail.

## 2  Setting and Requirements

We consider a finite-dimensional system of ordinary differential equations (ODEs) of the form

$$\dot{x} = f(x, \mu) \tag{1}$$

where $x \in \mathbb{R}^n$, $f : \mathbb{R}^n \times \mathbb{R} \mapsto \mathbb{R}^n$ is sufficiently smooth, and $\mu \in \mathbb{R}$ is the scalar parameter. The difference with the setup of standard continuation techniques lies in the fact that the evaluation of the right-hand-side $f$ is restricted according to (R1)–(R3).

We assume that (1) possesses a regular family $\Gamma$ of periodic orbits. Throughout the paper we make the following assumptions.

(A1) The family $\Gamma$ of periodic orbits is regular in the extended phase space. That is, there exists a smooth cylinder

$$\begin{aligned} \Gamma = \{&(x_{r,s}(\cdot), \mu_s, T_s) : r \in S^1, s \in [s_0, s_1]\} \\ &\subseteq C_p^1([-1, 0]; \mathbb{R}^n) \times \mathbb{R} \times \mathbb{R}^+, \end{aligned} \tag{2}$$

parameterized by $(r, s)$, such that $\partial_r x_{r,s} = T_s f(x_{r,s}, \mu_s)$. The notation $C_p^1([-1, 0]; \mathbb{R}^n) = \{x \in C^1([-1, 0]; \mathbb{R}^n) : x(-1) = x(0)\}$ refers to the space of all continuously differentiable periodic functions on the interval $[0, 1]$. Moreover, $\partial_r x_{r,s} = \dot{x}/T_s$. This means that the parameter $r$ is the phase shift along the periodic orbit and $s$ parameterizes the family $\Gamma$. We do not require that the system parameter $\mu$ is monotone in $s$, thus, allowing for $\Gamma$ to have folds.

3

(A2) We can apply control to the experiment. That is, instead of system (1) we consider the system

$$\dot{x}(t) = f(x(t), \mu) + g(x(t), \mu)u(t) \tag{3}$$

where $g : \mathbb{R}^n \mapsto \mathbb{R}^{n \times k}$, $u(t) \in \mathbb{R}^k$ ($k \leq n$), and $f$ is as defined for system (1).

(A3) We assume the existence of a successful periodic feedback control $u(t) = k_x(t, \mu)[x_0(t) - x(t)]$ of system (3). This means that we assume that there exists a $k_x \in \mathbb{R}^{k \times n}$ of period 1 in $t$ such that for all $(x_0, \mu_0, T_0)$ in the vicinity of the solution curve $\Gamma$ the system

$$\dot{x}(t) = f(x(t), \mu_0) + g(x(t), \mu_0)k_x(T_0 t, \mu_0)\left[x_0(T_0 t) - x(t)\right] \tag{4}$$

has a unique stable periodic solution near $x_0(T_0 \cdot) \in C^1([-T_0, 0]; \mathbb{R}^n)$.

In Sec. 3 we introduce various delay-difference equations that operate on the phase space of continuous functions on the *history interval* $[-1, 0]$ and prove that elements of $\Gamma$ are asymptotically stable for these delay-difference equations. To be consistent with the notation of history intervals, which is common in the treatment of delay equations (see Hale & Lunel [1993]), we choose the interval for the periodic function as $[-1, 0]$ in the definition of $\Gamma$ in Assumption (A1).

Assumption (A3) includes (i.e., is more restrictive than) the general assumption of feedback stabilizability of (3), which is typically required in control theory (Nam & Arapostathis [1992]). It is stronger in the sense that we not only assume that there exists a feedback control law that stabilizes a periodic orbit, but that we also know this feedback control law $k_x(t, \mu)$ in order to get a uniform stabilization along the solution curves. Assumption (A3) is trivially satisfied if $g(x)$ is a full-rank diagonal matrix. We may then choose $k_x(t, \mu)$ as a sufficiently large scalar constant to obtain, for example,

$$\dot{x}(t) = f(x(t), \mu_0) - k_x[x(t) - x_0(t)]. \tag{5}$$

# 3 Embedded Time-delayed Feedback Control

This section shows how one can embed time-delayed feedback control, a method to stabilize periodic orbits investigated by physicists interested in chaos control, into a continuation scheme. In this way we construct a new method that can be employed for continuation in experiments whenever the system parameter of interest (called $\mu$ in (1)) can be varied in real time. Section 3.1 introduces the basic idea of time-delayed feedback control as it has been investigated in the context of chaos control. Section 3.2 proves theoretically that our new method indeed increases the scope of the standard time-delayed feedback control. Section 3.3 demonstrates this fact with a numerical example of following periodic orbits through a fold of the family $\Gamma$, which is impossible with the standard time-delayed feedback control.

## 3.1 Time-delayed feedback control

Time-delayed feedback control has been introduced originally by Pyragas [1992]. The idea is to find unstable periodic orbits experimentally (typically, unstable periodic orbits that

are part of a chaotic attractor). It aims to stabilize the periodic orbit for fixed $\mu_0$ without knowing it by applying a control that depends on the difference between the current state $x$ and the state from some time ago. Socolar *et al.* [1994] extended this method, introducing a difference equation such that the combined system is a differential-difference equation for the two variables $x$ and $\tilde{x}$, which keeps track of the history of $\tilde{x}$:

$$\dot{x}(t) = T_0 f(x(t), \mu_0) + g(x(t), \mu_0) k_x(t, \mu_0) \left[ \tilde{x}(t) - x(t) \right]$$
$$\tilde{x}(t) = R\tilde{x}(t-1) + (1-R)x(t-1) \tag{6}$$

where $|R| < 1$. The phase space of system (6) is the space of continuous history segments $(x, \tilde{x}) \in C([-1, 0]; \mathbb{R}^n) \times C([-1, 0]; \mathbb{R}^n)$.

If the original uncontrolled system (1) at parameter $\mu_0$ has a periodic orbit $x_0(\cdot)$ of period $T_0$ then, after rescaling time, system (6) also has the periodic orbit $x(T_0\cdot) = \tilde{x}(T_0\cdot) = x_0(T_0\cdot)$. It has been observed experimentally and numerically in a number of papers (Bielawski *et al.* [1994]; Gauthier *et al.* [1994]; Kim *et al.* [2001]; Pyragas [1992, 2001]) that the periodic orbit $x = \tilde{x} = x_0$ in the coupled system (6) can be stable (and, thus, visible in experiments and simulations) even though $x_0$ is unstable in the original system (1). It has also been observed that choosing $R \in [0, 1)$ closer to 1 increases the parameter region where a given periodic orbit of (1) can be stabilized by (6), but at the cost of a slower attraction toward the stabilized orbit. The rate of attraction is bounded from below by the essential spectral radius $R$ of the linearization in the periodic orbit, imposed by the difference equation for $\tilde{x}$.

The scheme (6) is of interest for experimenters because it finds unstable periodic orbits without requiring knowledge about the linearization of the problem. Even more, the computation of the difference equation can often be implemented experimentally (for example, by two external mirrors in a laser experiment (see Tronciu *et al.* [2005]). The fact that system (6) does not involve any linearization suggests that finding periodic orbits with many unstable directions and of complicated shape or long period is likely to be impossible with this approach. However, if one is interested in exploring the boundaries of regions where stable oscillations occur then the control has to overcome only weak instabilities. This makes the scheme (6) suitable for bifurcation analysis and, possibly, direct continuation of bifurcations in experiments. Nakajima [2004] discusses conditions that guarantee that stabilization of periodic orbits is possible if one is close to a period-doubling or torus bifurcation boundary of a parameter region of stable periodic orbits for the case $R = 0$.

The main problems that one faces in the application of time-delayed feedback control as in (6) are the following.

(P1) The periodic orbit may only be locally stable in (6).

(P2) The period $T_0$ of the orbit has to be known in advance as it enters as the delay in the difference equation in the original time scale.

(P3) Periodic orbits of (1) with an odd number of positive unstable Floquet multipliers cannot be stable in (6); see Nakajima & Ueda [1998].

In the context of chaos control the problems (P1) and (P2) are tackled by relying on the presence of an ergodic attractor which contains infinitely many periodic orbits, one of which may have almost the chosen period. Pyragas [2001] introduces an approach to overcoming

5

problem (P3) by coupling an additional variable and equation into system (1). The approach of Pyragas [2001] increases the number of unstable Floquet multipliers to an even number before applying the time-delayed feedback control. However, this fails to converge uniformly in the vicinity of a fold (or saddle-node) bifurcation.

## 3.2 The embedding equations

This section shows that all of the problems (P1) to (P3) disappear when one embeds system (6) into a continuation of the family $\Gamma$ of periodic orbits. Our approach relies on the ability to vary the parameter $\mu$. We append two pairs of equations to (6) which

(E1) automatically determine the period of the periodic orbit,

(E2) introduce a parameter $s$ that parameterizes the family $\Gamma$ uniformly also near folds (compare with (2)), and

(E3) determine the system parameter $\mu$ and the periodic orbit $x(\cdot)$ depending on $s$.

**Determining the period** We first show that near a given *stable* periodic orbit we can automatically detect the period of all periodic orbits nearby by appending an equation for the unknown period $T$ that changes $T$ dynamically to fix the phase of the periodic orbit with respect to a given reference solution.

**Lemma 1.** *Let $(x_0(\cdot), \mu_0, T_0) \in \Gamma$ be a stable periodic orbit of (1). We define*

$$l_p(t)[x] := \int_{-1}^{0} \dot{x}_0(t+\theta)^T x(t+\theta)\, d\theta. \tag{7}$$

*Then for $\mu$ near $\mu_0$ and sufficiently small (in modulus) $k_{p,1} < 0$, $k_{p,2} > 0$ and $J_p > 0$ the system*

$$\begin{aligned}
\dot{x}(t) &= T f(x(t), \mu) \\
\dot{T} &= k_{p,1} \cdot l_p(t)[x] + k_{p,2} \cdot (\tilde{T} - T) \\
\dot{\tilde{T}} &= J_p \cdot (T - \tilde{T})
\end{aligned} \tag{8}$$

*has a stable periodic orbit $(x_\mu(\cdot), T_\mu, \tilde{T}_\mu)$ such that $x_\mu(\cdot)$ has period 1 and $T_\mu = \tilde{T}_\mu = const.$*

The triple $(x_\mu(\cdot), \mu, T_\mu)$ is an element of the family $\Gamma$ of periodic orbits of the original system (1). In fact, there exists a unique triple $(x_\mu(\cdot), T_\mu, \tilde{T}_\mu)$ which is a solution of (8) where $x_\mu(\cdot)$ has period 1 and $T_\mu = \tilde{T}_\mu = const.$ The only point that has to be shown is that this triple is stable w.r.t. (8) for suitably chosen parameters $k_{p,1}$, $k_{p,2}$, and $J_p$.

*Proof.* The linearization of system (8) in the unique solution $(x_\mu(\cdot), \mu, T_\mu)$ has the form

$$\begin{aligned}
\dot{y}(t) &= T A(t) y(t) + \dot{x}_\mu(t) \Theta(t) \\
\dot{\Theta}(t) &= k_{p,1} l_p(t)[y] + k_{p,2} \cdot (\tilde{\Theta}(t) - \Theta(t)) \\
\dot{\tilde{\Theta}}(t) &= J_p \cdot (\Theta(t) - \tilde{\Theta}(t))
\end{aligned} \tag{9}$$

where we use $(y, \Theta, \tilde{\Theta})$ as the linearization variables for $(x, T, \tilde{T})$ and $A(t) = \partial_1 f(x_\mu(t), \mu)$. In $k_{p,1} = k_{p,2} = J_p = 0$ it has a three-dimensional invariant center subspace corresponding to the Floquet multiplier 1 and a stable subspace of codimension three. The center subspace is spanned by the vectors $e_1$, $e_2$, $e_3$ given by

$$
\begin{aligned}
e_1 &= (y_1, \Theta_1, \tilde{\Theta}_1) \quad \text{where } y_1 = \dot{x}_\mu, \ \Theta_1 = \tilde{\Theta}_1 = 0, \\
e_2 &= (y_2, \Theta_2, \tilde{\Theta}_2) \quad \text{where } y_2 = 0, \ \Theta_2 = 1, \ \tilde{\Theta}_2 = 0, \\
e_3 &= (y_3, \Theta_3, \tilde{\Theta}_3) \quad \text{where } y_3 = \Theta_3 = 0, \ \tilde{\Theta}_3 = 1.
\end{aligned}
$$

The vector $e_2$ is a generalized eigenvector in the Jordan chain of $e_1$ for the Floquet multiplier 1 of the linearization (9). We observe that this invariant subspace does not change when varying $k_{p,1}$, $k_{p,2}$ and $J_p$. Thus, the linear stability is determined by the linearized time-1 (monodromy) map on the subspace of vectors of the form $ye_1 + \Theta e_2 + \tilde{\Theta} e_3$. If $k_{p,1} = 0$, $k_{p,2} \geq 0$ and $J_p > 0$ this monodromy map still has an eigenvalue 1 of algebraic multiplicity two and a third eigenvalue $\exp(-k_{p,2} - J_p)$, which has modulus less than 1. Expansion of the location of the two eigenvalues $\lambda$ near 1 in $k_{p,1}$ for $k_{p,1} \neq 0$ gives

$$
\lambda(k_{p,1}) = 1 \pm \sqrt{d_0}\sqrt{k_{p,1}} + \frac{d_1}{4}k_{p,1} + O(k_{p,1}^2) \tag{10}
$$

where

$$
\begin{aligned}
d_0 &= \frac{J_p}{2k_{p,2} + J_p} l_p(0)[\dot{x}_\mu] > 0 \\
d_1 &= \frac{J_p^2 + J_p k_{p,2} + k_{p,2}(1 - \exp(-k_{p,2} - J_p))}{(k_{p,2} + J_p)^2 (1 - \exp(-k_{p,2} - J_p))} > 0.
\end{aligned}
$$

Thus, if $k_{p,1}$ is negative and sufficiently small then the eigenvalues $\lambda(k_{p,1})$ are shifted into the unit circle by increasing $k_{p,2}$ and keeping $J_p$ fixed. $\qquad\square$

Changing $k_{p,1}$ from zero to a non-zero value converts system (8) into a delay differential equation because $l_p(t)$ depends on the history of $x$. This 'creates' infinitely many eigenvalues near 0. The requirement that none of these crosses the circle of a given radius less than 1 adds another restriction on the size of $|k_{p,1}|$.

The location of the other eigenvalues of the monodromy operator remains unchanged when decreasing $k_{p,1}$ from zero. This means that we can extend Lemma 1 to periodic orbits with critical stability.

**Definition 2.** *We call a periodic orbit* critically stable (critical) *if all of its Floquet multipliers $\lambda_j$ satisfy*

- $|\lambda_j| \leq 1$,

- *if $|\lambda_j| = 1$ and $\lambda_j \neq 1$ then $\lambda_j$ has algebraic multiplicity one,*

- *if $\lambda_j = 1$ then it has algebraic multiplicity of at most two.*

*The Floquet multipliers on the unit circle are called* critical.

**Corollary 3.** *Let $(x_0(\cdot), \mu_0, T_0) \in \Gamma$ be a critically stable periodic orbit of (1). Then $(x_0(\cdot), \mu_0, T_0)$ is also a critically stable periodic orbit of system (8) with sufficiently small (in modulus) $k_{p,1} < 0$, $k_{p,2} > 0$ and $J_p > 0$. The algebraic multiplicity of the Floquet multiplier $1$ is decreased by one in (8) compared to (1).*

If the Floquet multiplier 1 of $(x_0(\cdot), \mu_0, T_0)$ has multiplicity one in (1) then Corollary 3 implies that $(x_0(\cdot), \mu_0, T_0)$ has no Floquet multiplier 1 at all in (8).

The particular choice of the functional $l_p(t)$ in (7) plays only a role in guaranteeing that $l_p(t)[\dot{x}_\mu] > 0$ for $\mu \approx \mu_0$. Thus, we know that $k_{p,1}$ has to be negative. The same functional is chosen to provide a phase condition in the numerical continuation of periodic orbits using classical boundary value solvers (for example, in AUTO). In fact, any choice of $l_p(t)$ which implies that $l_p(t)[\dot{x}_0]$ is not identically zero gives the same result. Lemma 1 implies that we can automatically determine the period of orbits of the family $\Gamma$ by solving (8) at least along stable parts of the family.

**Pseudo-arclength embedding** Similar to the extension of the delay-difference feedback control scheme (6) by a phase equation determining the period, we add an equation replacing the actual system parameter $\mu$ by a pseudo-arclength parameter. Suppose that $z_0 = (x_0(\cdot), \mu_0, T_0) \in \Gamma$ is a periodic orbit of the general system (1) and that $z_t = (x_t(\cdot), \mu_t, T_t)$ is the tangent to $\Gamma$ in $z_0$. We consider the linear functional $l_a(t)[x, \mu, T]$ of the form

$$l_a(t)[x, \mu, T] = \int_{-1}^{0} x_t(t+\theta)^T x(t+\theta) \, d\theta \; + \; \mu_t \mu + T_t T \tag{11}$$

and the constant term

$$l_s = l_a(0)[x_s, \mu_s, T_s]$$

where $z_s = (x_s(\cdot), \mu_s, T_s)$ is given by $z_s = z_0 + s z_t$ and $s$ is sufficiently small. The particular form (11) of $l_a(t)$ is used in the classical numerical continuation to determine the system parameter from the pseudo-arclength along a solution curve (Doedel *et al.* [1998]; Kuznetsov [2004]). If $z = (x, \mu, T) \in \Gamma$ satisfies $l_a(0)[x, \mu, T] = l_s$ then $(x, \mu, T) - (x_s, \mu_s, T_s)$ is orthogonal to the tangent of the solution family $\Gamma$, thus, guaranteeing that the distance between the two points $(x, \mu, T)$ and $(x_0, \mu_0, T_0)$ on the solution curve $\Gamma$ is $s + O(s^2)$.

As we show now, introducing a pseudo-arclength parameter and a differential equation for $\mu$ results in a control scheme that is successful and fixes $\mu$ by stabilizing it dynamically, at least near all critically stable periodic orbits. Thus, this control scheme works uniformly near all stability boundaries of $\Gamma$ of codimension one, including folds. The idea to impose a pseudo-arclength condition dynamically as a control has been considered also by Siettos *et al.* [2004] (however in the context of continuation of equilibria, which removes the presence of a delay).

**Lemma 4.** *Let $z_0 = (x_0, \mu_0, T_0)$ be a critically stable periodic orbit of (1). Suppose that the stabilizability assumption (A3) is satisfied for $z_0$ in such a way that all critical Floquet multipliers $\lambda_{c,j}$ different from $1$ of the periodic orbit $x_0(T_0 \cdot)$ of*

$$\dot{x}(t) = f(x(t), \mu) + g(x(t), \mu) \cdot \alpha k_x(t, \mu_0)[x_0(T_0 t) - x(t)] \tag{12}$$

8

*satisfy*

$$\text{Re}\left(\bar{\lambda}_{c,j} \cdot \left[\frac{\partial \lambda_{c,j}}{\partial \alpha}\right]\Big|_{\alpha=0}\right) < -\rho < 0 \tag{13}$$

*for a positive constant $\rho$ and all sufficiently small $\alpha$. Choose the parameters $k_{p,1}$, $k_{p,2}$ and $J_p$ as required in Lemma 1. Then there exist parameters $\alpha > 0$, $k_a$ (sufficiently small) and $R$ (sufficiently close to 1) such that the system*

$$\dot{x}(t) = Tf(x(t),\mu) + g(x(t),\mu)\,\alpha k_x(t,\mu)\,[\tilde{x}(t) - x(t)] \tag{14}$$

$$\dot{\mu} = k_a \cdot (l_a(t)[x,\mu,T] - l_s) \tag{15}$$

$$\dot{T} = k_{p,1} \cdot l_p(t)[x] + k_{p,2} \cdot (\tilde{T} - T) \tag{16}$$

$$\tilde{x}(t) = R\tilde{x}(t-1) + (1-R)x(t-1) \tag{17}$$

$$\dot{\tilde{T}} = J_p \cdot (T - \tilde{T}) \tag{18}$$

*has a stable solution $(x(\cdot), \tilde{x}(\cdot), \mu, T, \tilde{T})$ where $x(\cdot) = \tilde{x}(\cdot)$ have period one and $\mu = const$, $T = \tilde{T} = const$ for all sufficiently small $s$.*

Condition (13) is more specific than the controllability condition (A3) in the sense that it requires the feedback control law $k_x$ to be such that it shifts critical Floquet multipliers into the unit circle with positive velocity $\rho$ when it is "switched on" (that is, $\alpha$ is increased from 0). The derivative with respect to the parameter $\alpha$ in (13) is well defined since the critical Floquet multipliers different from 1 are assumed to be simple.

The fact that system (14)–(18) has a solution $(x(\cdot), \tilde{x}(\cdot), \mu, T, \tilde{T})$ with the desired properties is clear by construction. Namely $(x(\cdot), \tilde{x}(\cdot), \mu, T, \tilde{T}) = (x(\cdot), x(\cdot), \mu, T, T)$ where the triple $(x(\cdot), \mu, T)$ is the element of $\Gamma$ with pseudo-arclength distance $s$ from $z_0$, which is unique for non-zero $k_a$ and $k_{p,1}$ and sufficiently small $s$. The only open question is the dynamical stability of this solution. Importantly, the parameters can be chosen uniform for whole compact connected components of $\Gamma$ which are either stable or critically stable.

*Proof.* (Lemma 4) It is sufficient to prove the linear stability of the periodic solution for $s = 0$. We know that the regular family $\Gamma$ provides also solutions of system (14)–(18) for small $s$. Since the perturbation to a nonzero $s$ is regular these solutions are locally unique and also stable.

Let us consider the subsystem (14)–(16)/(18) where we replace the variable $\tilde{x}$ in (14) by $x_0$ (the $x(\cdot)$-component of $z_0$). This system is a delay differential equation with periodic forcing of period one. The stability of the periodic solution $x = x_0$, $\mu = \mu_0$, $T = \tilde{T} = T_0$ of period one is determined by the Floquet multipliers of the linearization of the time-1 map in the associated fixed point. All non-zero Floquet multipliers are described as roots $\lambda$ of a characteristic equation of the form $h(\lambda) = 0$ where $h$ is analytic in $\lambda$ for $\lambda \in \mathbb{C} \setminus \{0\}$ (see Szalai *et al.* [2004]). The characteristic function $h$ has infinitely many roots with 0 as their only accumulation point. We also take into account the dependence of $h$ on the parameters $k_{p,1}$, $k_{p,2}$, $\alpha$ and $k_a$ (which is smooth). For $\alpha = k_a = k_{p,1} = k_{p,2} = 0$ the roots of $h$ are the Floquet multipliers of $x_0$ as an element of $\Gamma$. In addition, there is one root of $h$ at $\lambda_{\tilde{T}} = \exp(-J_p - k_{p,2})$ due to the decoupled equation for $\tilde{T}$. Furthermore, the multiplicity of the root $\lambda = 1$ of $h$ is exactly three due to the regularity of the family of periodic orbits

$\Gamma$ in (1), one for the trivial Floquet multiplier of $x_0$, one for the equation $\dot{T} = 0$, and one for the equation $\dot{\mu} = 0$ (which also accounts for folds of $\Gamma$ with respect to $\mu$). As shown in Lemma 1 and Corollary 3, choosing $k_{p,1} < 0$, $k_{p,2} > 0$ and $J_p > 0$ sufficiently small reduces the multiplicity of the root 1 of $h$ to one, creating instead the roots $\lambda(k_{p,1})$ as described by expression (10), which have modulus less than one and non-zero imaginary part. From now on we keep $k_{p,1}$, $k_{p,2}$ and $J_p$ fixed, such that $h$ depends only on $\lambda$ and the parameters $k_a$ and $\alpha$. Let us express this dependence explicitly by using the notation $h(\lambda, \alpha, k_a)$.

The function $h(\cdot, 0, 0)$ has only simple roots on the unit circle, one of them at 1, by the assumption of critical stability. Let us denote these simple roots by $\lambda_{c,j}$ where $j = 1 \ldots k$ ($k \geq 1$ because $\lambda_{c,1} = 1$ is a root of $h(\cdot, 0, 0)$). Due to their simplicity the roots $\lambda_{c,j}$ are uniquely defined for all sufficiently small $\alpha$ and $k_a$ and the dependence of $\lambda_{c,j}$ on $k_a$ and $\alpha$ is smooth. All other roots lie inside the unit circle. We denote

$$a_j := \left.\frac{\partial \lambda_{c,j}}{\partial \alpha}\right|_{\alpha = k_a = 0} = -\frac{\partial_2 h(\lambda_{c,j}, 0, 0)}{\partial_1 h(\lambda_{c,j}, 0, 0)}.$$

By assumption (13) we have for $j \neq 1$

$$\mathrm{Re}(\bar{\lambda}_{c,j} a_j) = \frac{\partial |\lambda_{c,j}|}{\partial \alpha} < 0. \tag{19}$$

The characteristic function of the full linearized system (14)–(18) with $R \in (0, 1)$ in $x = \tilde{x} = x_0$, $\mu = \mu_0$, $T = \tilde{T} = T_0$ is given by

$$\tilde{h}(\lambda, \alpha, k_a) = h(\lambda, \alpha \cdot \frac{\lambda - 1}{\lambda - R}, k_a)$$

which is defined and analytic for $\lambda \in \mathbb{C} \setminus \{0, R\}$. The value $\lambda = R$ is essential spectrum of the linearization induced by (17). Those roots of $\tilde{h}(\cdot, 0, k_a)$ that are different from $R$ are identical to the roots of $h(\cdot, 0, k_a)$. For $\alpha \neq 0$ but sufficiently small all roots of $\tilde{h}(\cdot, \alpha, k_a)$ outside of the circle around 0 of radius $(1 + R)/2$ are small perturbations of roots of the roots of $h(\cdot, \alpha, k_a)$. In particular, all roots of $\tilde{h}(\cdot, \alpha, k_a)$ lie inside the unit circle except the $k$ roots $\tilde{\lambda}_{c,j}$ which are perturbations of $\lambda_{c,j}$ of order $O(\alpha)$, depending smoothly on $\alpha$ and $k_a$.

For $k_a = 0$ and small $\alpha$ the modulus of the roots $\tilde{\lambda}_{c,j}$ satisfies

$$|\tilde{\lambda}_{c,j}|^2 = 1 + \alpha \cdot 2 \, \mathrm{Re} \left[ \bar{\lambda}_{c,j} a_j \frac{\lambda_{c,j} - 1}{\lambda_{c,j} - R} \right]_{\alpha = 0} + O(\alpha^2). \tag{20}$$

All $\lambda_{c,j}$ except $\lambda_{c,1}$ have a positive distance from 1. Thus, due to (19) we can choose $R \in (0, 1)$ sufficiently close to 1 such that the coefficient $\mathrm{Re}[\bar{\lambda}_{c,j} a_j (\lambda_{c,j} - 1)/(\lambda_{c,j} - R)]$ is negative for all $j > 1$. Consequently, for a sufficiently small non-zero value of $\alpha$ all roots $\tilde{\lambda}_{c,j}$ for $j > 1$ are in the interior of the unit circle according to (20). We keep $\alpha$ and $R$ fixed from now on. The only root of $\tilde{h}(\cdot, \alpha, 0)$ that is not inside the unit circle is $\tilde{\lambda}_{c,1}$, which is equal to 1 independently of $\alpha$.

Finally, we notice that for $k_a \neq 0$ the function $h(1, 0, k_a) = \tilde{h}(1, 0, k_a)$ is non-zero because $(x_0, \mu_0, T_0)$ is a unique regular periodic orbit of system (14)–(16) for $\alpha = 0$ and non-zero

$k_a$ and $k_{p,1}$. Since $k_a$ enters the right-hand-side linearly, this implies that $\partial_3 \tilde{h}(1, \alpha, 0) \neq 0$. Thus,

$$b_0 = \left. \frac{\partial \tilde{\lambda}_{c,1}}{\partial k_a} \right|_{k_a=0} = -\frac{\partial_3 \tilde{h}(1, \alpha, 0)}{\partial_1 \tilde{h}(1, \alpha, 0)} \neq 0$$

where $b_0 \in \mathbb{R}$. Hence, if we choose $k_a$ non-zero with the opposite sign of $b_0$ the root $\tilde{\lambda}_{c,0}$ is shifted into the unit circle. Furthermore, if $k_a$ is sufficiently small then all other roots of $\tilde{h}(\cdot, \alpha, k_a)$ stay inside the unit circle. This implies the linear stability of the solution $(x_0, \mu_0, T_0, x_0, T_0)$ of system (14)–(18). $\qquad \square$

The choice of control parameters in system (14)–(18) is roughly $0 < -k_{p,1} \ll 1$, $0 < k_{p,2} \ll 1$, $R \in (0,1)$ with $(1-R) \ll 1$. Then $\alpha > 0$ should be small compared to $(1-R)$, $|k_{p,1}|$ and $k_{p,2}$, and $|k_a| \ll \alpha$. The sign of $k_a$ depends on the problem dependent quantity $b_0$. However, along a regular family $\Gamma$ this sign can be chosen uniformly. Thus, it is not necessary to change it during a continuation.

**Outline of Algorithm**  The statement of Lemma 4 allows one to successively continue the family $\Gamma$ within the region of stability but also up to and slightly beyond its codimension one bifurcations. (In practice one observes that, when the instability becomes stronger or more unstable directions are present, one has to start tuning the method parameters along the branch in a problem-dependent way.) The basic outline of the continuation is as follows.

(S1) *Initialization*: Suppose a dynamically stable periodic orbit $z = (x(\cdot), \mu, T)$ is given or has been found by running the original system (1). Choose an initial direction $\mu_t = \pm 1$ and a step size $s \ll 1$. Initialize $z_0 = (x_0, \mu_0, T_0) = z$ and $z_t = (0, \mu_t, 0)$ (thus, defining $l_p(t)$ and $l_a(t)$). Determine the sign of the parameter $k_a$ (called $k_{a,1}$ in (21)) by trial and error.

(S2) *Predictor*: Choose $z_s = z_0 + s z_t$, defining $l_s$.

(S3) *Correction*: Run the dynamical system

$$
\begin{aligned}
\dot{x}(t) &= T f(x(t), \mu) + g(x(t), \mu) \, k_x(t, \mu) \, [\tilde{x}(t) - x(t)] \\
\tilde{x}(t) &= R\tilde{x}(t-1) + (1-R)x(t-1) \\
\dot{T} &= k_{p,1} \cdot l_p(t)[x] + k_{p,2} \cdot (\tilde{T} - T) \\
\dot{\tilde{T}} &= J_p \cdot (T - \tilde{T}) \\
\dot{\mu} &= k_{a,1}(l_a(t)[x, \mu, T] - l_s) + k_{a,2} \cdot (\tilde{\mu} - \mu) \\
\dot{\tilde{\mu}} &= J_a \cdot (\mu - \tilde{\mu})
\end{aligned}
\tag{21}
$$

with the initial conditions $\tilde{x} = x_s$, $T = \tilde{T} = T_s$, $\mu = \tilde{\mu} = \mu_s$ and $x = x_0$. The system has a stable periodic orbit of period one satisfying $x = \tilde{x}$, $\mu = \tilde{\mu} = const$ and $T = \tilde{T} = const$. If $s$ is sufficiently small we are in its basin of attraction, so we wait for the transients to decay below a given tolerance.

11

(S4) *Update*: $z_{\text{new}} = (x, \mu, T)$ and $z_t = z_{\text{new}} - z_0$, normalized to $\|z_t\| = 1$, and, finally, $z_0 = z_{\text{new}}$. Then repeat from step (S2).

The steps follow a classical pseudo-arclength continuation scheme using a secant predictor. The main difference to classical numerical tools such as AUTO is that we stabilize the periodic orbit dynamically in the corrector step instead of solving for it directly by Newton iterations. Importantly, it is not necessary to set an initial value of $x$ in system (21) because $x$ has already the initial condition $x_0$ from the previous step, which is, for sufficiently small $s$, within the basin of attraction. This property is a practical advantage if one wants to use continuation in an experimental setting.

The capability to continue beyond codimension-one stability boundaries includes folds according to Lemma 4. This means in particular that the restriction on the number of unstable positive Floquet multipliers (see problem (P3) on page 5 and Nakajima & Ueda [1998]; Pyragas [2001]) does not apply to system (21). The fact that none of the steps (S1) to (S4) in the algorithm outline involves an estimate or computation of the linearization of the system is also of particular appeal in an experimental context. Lemma 4 proves that the correction indeed stabilizes a periodic orbit in the special case $k_{a,2} = 0$.

Furthermore, the accuracy and speed requirements for the time integration of $T$, $\tilde{T}$, $\mu$ and $\tilde{\mu}$ are low. Any consistent scheme with a step size that preserves the stability of the original solution is sufficient because one is not interested in the details of the transient behavior of $T$, $\tilde{T}$, $\mu$ and $\tilde{\mu}$ but only in their equilibrium values.

## 3.3  Example I — semiconductor laser with optical injection

In this section we use a numerical example to illustrate that the pseudo-arclength embedding of the extended time-delayed feedback stabilization is indeed not affected by restrictions on the odd-number property of periodic orbits (see problem (P3)). Moreover, and this is different to the construction of Pyragas [2001], the extended system is uniformly dynamically stable in the vicinity of fold (saddle-node) bifurcations of periodic orbits.

The example system, a model describing a semiconductor laser subject to optical injection, has been studied extensively as a prototype for complicated dynamics in a simple dynamical system; see Wieczorek *et al.* [2005] for an overview. Many of the features described by Wieczorek *et al.* [2005] are of practical relevance in the application of lasers. Moreover, there is excellent agreement between the two-parameter bifurcation diagram of the mathematical model and experimental measurements. The model consists of a system of two ordinary differential equations, one for the complex electric field $E \in \mathbb{C}$ (the light) and one for the carrier density $n \in \mathbb{R}$ (the number of electron-hole pairs in the semiconductor material):

$$
\begin{aligned}
\dot{E} &= K + ((1 + i\alpha)n/2 - i\omega)E \\
\dot{n} &= -2\Gamma n - (1 + 2Bn)(|E|^2 - 1).
\end{aligned}
\tag{22}
$$

The parameter $K$ represents the injection strength relative to the pumping current of the laser, and $\omega$ the frequency detuning between the injected light and the natural frequency of the free-running laser. These two parameters are the primary bifurcation parameters. The other parameters (the so-called linewidth-enhancement factor $\alpha$, the carrier decay rate $\Gamma$ and
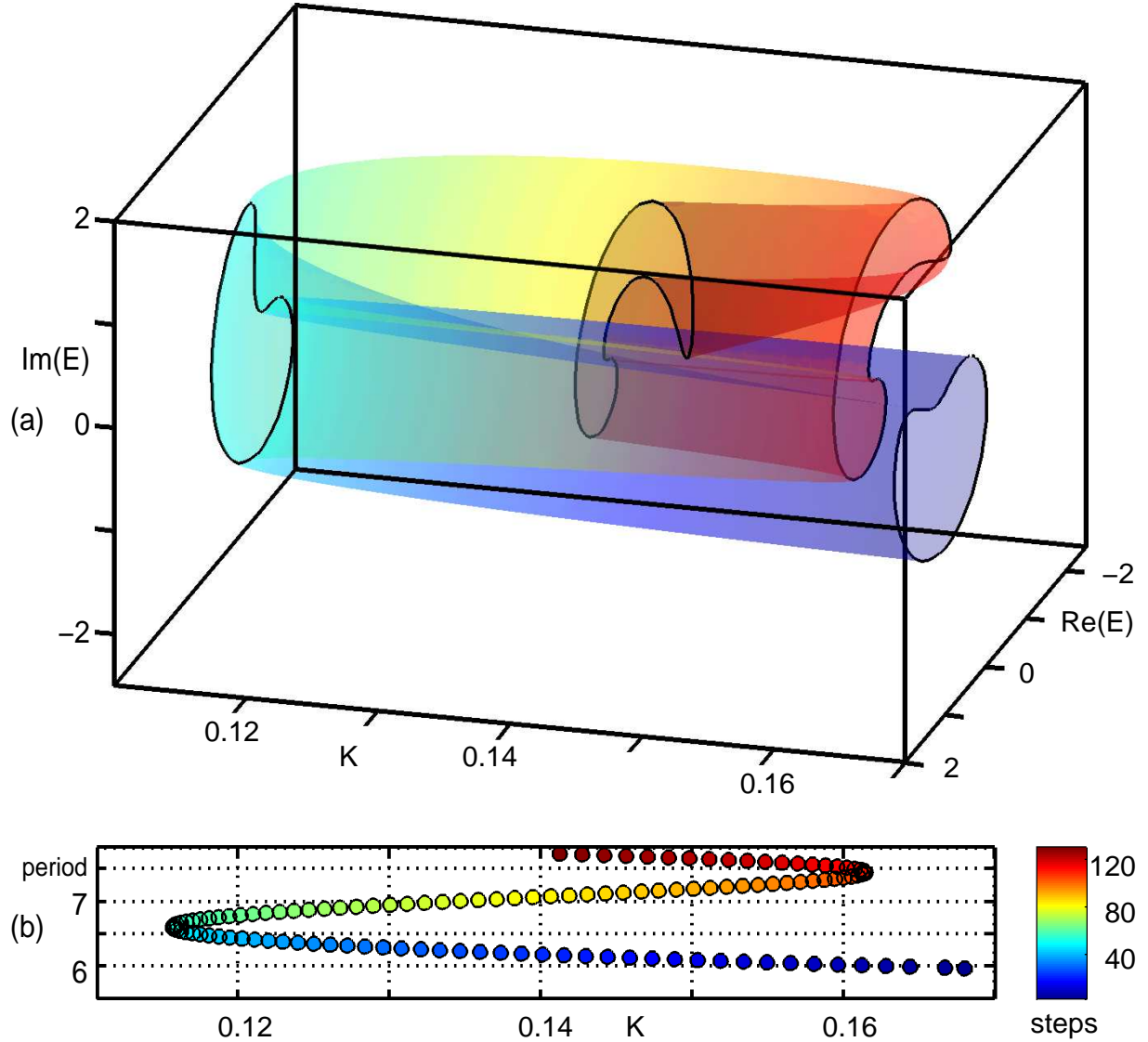
Figure 1: Continuation in $K$ of the family of periodic orbits in the laser with optical injection (22) for $\omega = 0.85$, $\alpha = 2$, $B = 0.015$ and $\Gamma = 0.035$. Both panels show the one-parameter bifurcation diagram for the parameter $K$ between 0.1 and 0.17. Panel (a) plots the variable $E$, and panel (b) the period. The orbits highlighted in black in panel (a) are the first and the last of the continuation and the two fold orbits. The color code (ranging from blue to red) indicates the step number along the continued branch.

the gain $B$) are material constants and difficult to vary or even measure in an experiment. We fix them at realistic values: $\alpha = 2$, $B = 0.015$ and $\Gamma = 0.035$.

System (22) has been studied extensively with numerical continuation using AUTO; see Wieczorek *et al.* [2005] for an overview. One phenomenon reported and investigated first by Wieczorek *et al.* [2000] was the coexistence of several stable attractors which is related to the presence of cusps of periodic orbits in the two-parameter plane. If one chooses a line in the parameter plane that passes nearby a cusp one typically observes two successive fold
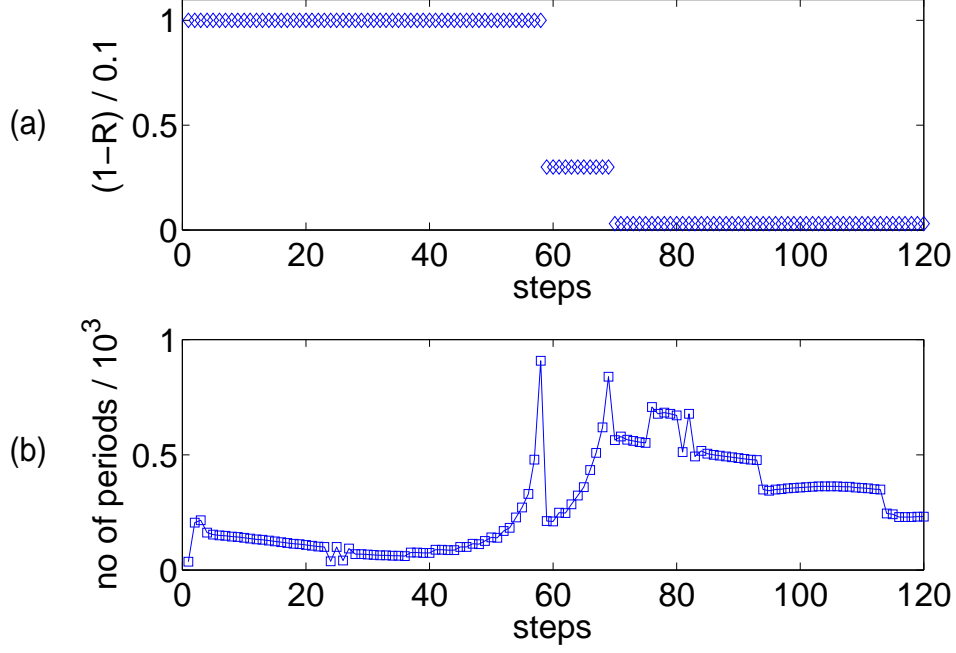
Figure 2: Convergence of time-delayed feedback control along the family of periodic orbits of Fig. 1. Panel (a) shows the factor $(1 - R)$ that was chosen in each step. Panel (b) shows the time that the transients took to decay to $10^{-5}$ for each step along the continuation.

bifurcations. This scenario is our test case to demonstrate that the stabilization (21) works uniformly near fold bifurcations of periodic orbits. We fix $\omega = 0.85$, choose $K$ as our system parameter and assume $g = I$, resulting in

$$
\begin{aligned}
\dot{E} &= T \cdot (K + ((1 + i\alpha)n/2 - i\omega)E) - k_x(E - \tilde{E}) \\
\dot{n} &= T \cdot (-2\Gamma n - (1 + 2Bn)(|E|^2 - 1)) - k_x(n - \tilde{n}) \\
\tilde{E}(t) &= R\tilde{E}(t - 1) + (1 - R)E(t - 1) \\
\tilde{n}(t) &= R\tilde{n}(t - 1) + (1 - R)n(t - 1) \\
\dot{T} &= k_{p,1}l_p(t)[E, n] - k_{p,2}(T - \tilde{T}) \\
\dot{K} &= k_{a,1}l_a(t)[E, n, K, T] - k_{a,2}(K - \tilde{K}) \\
\dot{\tilde{T}} &= (1 - R_p)(T - \tilde{T}) \\
\dot{\tilde{K}} &= (1 - R_a)(K - \tilde{K})
\end{aligned}
\tag{23}
$$

for the dynamical system (21) in the corrector step. The initial value is the result of a simulation for $K = 0.17$, which gives a stable periodic orbit. We choose $\mu_t = -1$ (that is, decreasing $K$) as our initial direction and then apply the continuation scheme (S1)–(S4) repeatedly.

The results are shown in Fig. 1 and Fig. 2. Figure 1 shows the $E$-profile in panel (a), and the period $T$ in panel (b) versus the parameter $K$ for the family $\Gamma$ of periodic orbits computed by this procedure. The two folds of the family are clearly visible in both panels and occur at $K \approx 0.116$ and $K \approx 0.161$. Figure 2(b) shows for each step the rescaled time

14

(number of periods) that the transients needed to decay to a level of $10^{-5}$ in the corrector step (S3). Figure 2(b) is evidence that the folds (occurring at the points 46 and 100 in Fig. 2(b)) do not impede the successful stabilization. Apparently the system converges much slower than numerical methods that are based on Newton iterations. The control parameters $k_x = 2$, $k_{a,2} = k_{p,2} = 1$, $k_{p,1} = -0.1$, $k_{a,1} = 10^{-2}$ were not adapted but chosen uniformly along the continuation. The potential for improvement of the convergence lies in an appropriate adaptation of the available control parameters without the need to compute a full linearization. The parameter $(1 - R)$ (shown in Fig. 2(a)) was chosen as $10^{-1}$ initially and then decreased whenever the transients had not died down after 1000 periods. In the range of applicability of Lemma 4 (slightly beyond point 46 in Fig. 2(a)) $(1 - R)$ is uniformly 0.1.

# 4  Preconditioning with Estimated Derivatives

The extended time-delayed feedback control scheme (6) can, in the limit $(1 - R) \to 0$, be viewed as a Picard-type iteration to find periodic orbits. It requires no computation of the linearization of the system. The embedding into a continuation scheme has the advantage that one unstable Floquet multiplier can be stabilized if it is sufficiently close to the unit circle. We describe in this section how one can make the approach introduced in the Sec. 3 more robust and universal if one is prepared to spend more effort. A similar idea has been pursued by Baba *et al.* [2002] who discuss preconditioning techniques for time-delayed feedback using the left and right leading eigenvectors of the Floquet problem corresponding to the linearization of the original system (1) in the target orbit. We introduce the scheme in Sec. 4.1 and use it in Sec. 4.2 to compute the canard periodic orbits in the stiff Van der Pol oscillator with constant forcing.

## 4.1  Preconditioning operator

Instead of the real number $R$ in (6) we choose a general operator acting on $\tilde{x} - x$. More precisely, assumption (A3), requiring controllability, implies that there exists a smooth map

$$X : C_p^1([-1, 0]; \mathbb{R}^n) \times \mathbb{R} \times \mathbb{R} \mapsto C_p^1([-1, 0]; \mathbb{R}^n)$$

mapping the control input $x_0(\cdot)$, parameter $\mu_0$, and period $T_0$ of $x_0$ to a unique stable periodic orbit $x(\cdot) = y(T_0 \cdot)$ of the periodically forced system

$$\dot{y}(t) = f(y(t), \mu_0) + g(y(t), \mu_0)k_x(T_0 t, \mu_0)\left[x_0(T_0 t) - y(t)\right] \qquad (24)$$

where $x$ has period 1 and $y$ has period $T_0$. This map satisfies $X(x_0, \mu_0, T_0) = x_0$ for any element $(x_0, \mu_0, T_0)$ of the family $\Gamma$ of periodic orbits of the original uncontrolled system (1). Ideally, the operator $R$ should approximate the inverse of the linearization of the map $X(x, \mu, T) - x$ with respect to $x$ in $x = x_0$. This would result in quadratic convergence of the iteration. Since any operator $R$ that is more complicated than a multiplication by a real number is too costly to be evaluated continuously (especially during an experiment) we apply the difference equation only at discrete times. This results in the following system, which

is solved by a Quasi-Newton iteration in the corrector step (S3) as part of the algorithm (S1)–(S4):

$$0 = \tilde{x} - X(\tilde{x}, \mu, T) \tag{25}$$
$$0 = l_a(0)[\tilde{x}, \mu, T] - l_s \tag{26}$$
$$0 = l_p(0)[\tilde{x}] \tag{27}$$

for the variables $\tilde{x} \in C_p^1([-1, 0]; \mathbb{R}^n)$, $\mu$ and $T$. Thus, the steps (S1)—(S4) are now formally identical with classical numerical continuation methods such as AUTO (see Doedel *et al.* [1998]; Kuznetsov [2004]). The remaining difficulty is that (25) requires the evaluation of the map $X(\tilde{x}, \mu, T)$. This evaluation of $X$ involves the following two steps.

(X1) Set the control target $x_0$ to $\tilde{x}$ in (24) with the parameters $\mu_0 = \mu$ and $T_0 = T$.

(X2) According to the assumptions (A1)–(A3) the (periodically forced) dynamical system (24) has a stable periodic orbit $y$ of period $T_0$. We run the dynamical system (24) until it has reached its periodic state, which we record (after rescaling time by $T_0$) as the expression of $X(\tilde{x}, \mu, T)$.

Again, this procedure does not require setting an initial value of (24) during a continuation. The extended time-delayed feedback control method (21) is equivalent to solving (25)–(27) with a relaxed fixed point iteration (after premultiplying (27) by $-1$ and (26) by a problem-dependent sign).

Finding the linearization of $X$ is difficult because the Jacobian $\partial_1 X$ is dense, which makes it impossible to obtain $\partial_1 X$ directly by finite differences. If one assumes that the map $X$ has been generated by a system of the form (24) of dimension $n$ then the partial derivatives of $X$ with respect to its first argument in a given point $(x_0, \mu_0, T_0)$ with $X(x_0, \mu_0, T_0) = x_0$ satisfy

$$\frac{d}{dt}\frac{\partial X}{\partial \tilde{x}}(t) = A(t)\frac{\partial X}{\partial \tilde{x}}(t) + B(t)\left(\tilde{x}(t) - \frac{\partial X}{\partial \tilde{x}}(t)\right). \tag{28}$$

for

$$A(t) = \partial_1 f(x_0(T_0 t), \mu_0) - g(x_0(T_0 t), \mu_0)k_x(t, \mu_0),$$
$$B(t) = g(x_0(T_0 t))k_x(t, \mu_0).$$

This allows us to compute the unknown matrices $A(t)$ and $B(t)$ by recording $X$ for at least $2n$ different small deviations $x_0 + \delta\tilde{x}$. Then the derivative $\partial_1 X$ can be obtained by the relation

$$\partial_1 X = [B(\theta) + \partial_\theta - A(\theta)]^{-1} B(\theta) \tag{29}$$

on the space $C_p^1([-1, 0]; \mathbb{R}^n)$ of periodic functions. This approach is common in control methods based on the Ott-Grebogi-Yorke (OGY) approach (see, for example, Christini *et al.* [1996]). However, in the OGY approach the instances of $X$ are typically recorded over chaotic time series. Feo & Maggio [2003] have carried out bifurcation analysis in a real implementation of a Colpitts oscillator electronic circuit based on a system identification of

16

$A(t)$ and $B(t)$. A major problem of this indirect computation of the coefficients $A(t)$ and $B(t)$ is that it can be ill-posed and requires the differentiation of a time profile with respect to time and the small deviation $\delta\tilde{x}$.

Alternatively, a decomposition into Fourier modes gives rise to a representation of $X$ in the basis of the Hilbert space $\mathbb{L}^2$. A (Quasi-) Newton iteration for system (25)–(27), projected on the leading Fourier modes, can then be combined with the time-delayed feedback control scheme (21) resulting in a Newton-Picard type iteration. Finding efficient and robust ways to obtain an approximation of the linearization of $X$ that are also feasible in experiments is an open problem for future work.

## 4.2 Example II — Canard periodic orbits in the stiff Van der Pol oscillator with constant forcing

This section demonstrates that a continuation of system (25)–(27) allows us to find phenomena without evaluations of the right-hand-side that have so far been difficult to track due to their extreme sensitivity. We also test the approximation (28) of the Jacobian by comparing it to the reference solution obtained by using the direct analytical Jacobian in the previous point along the branch.

A classical example of periodic orbits that are very sensitive to perturbations (and, hence, difficult to find in experiments) is the family of so-called canard periodic orbits in the Van der Pol (FitzHugh-Nagumo) oscillator; see for example Dumortier & Roussarie [1996]; Guckenheimer *et al.* [2003]; Krupa & Szmolyan [2001]. This is a slow-fast two-dimensional system of ODEs, governed by the equations

$$\begin{aligned}
\dot{x} &= \varepsilon(a - y) \\
\dot{y} &= x + y - \frac{y^3}{3}.
\end{aligned} \tag{30}$$

The parameter $\varepsilon$, which is positive and small, determines the separation of the time-scales of $x$ and $y$. The system has the slow manifold $x = y^3/3 - y$ which is transversally stable for $|y| > 1$ and unstable for $|y| < 1$. The parameter $a$ (a constant forcing) determines the dynamics on the slow manifold, giving rise to a fixed point $(x_f, y_f) = (a^3/3 - a, a)$. The fixed point is stable for $|a| > 1$, unstable for $|a| < 1$ and undergoes a Hopf bifurcation at $a = \pm 1$. For $a \in (-1, 1)$ there exists a family $\Gamma$ of stable periodic orbits, which can be parameterized by $a$, that is, $\Gamma = \{(x_a(\cdot), T_a) : a \in (-1, 1)\} \subset C_p^1([-1, 0]; \mathbb{R}^2) \times \mathbb{R}$ (see Hirsch & Smale [1974]). However, for small $\varepsilon$ the dependence of $(x_a(\cdot), T_a)$ on $a$ is extremely sensitive in an interval $\mathcal{I}_c(\varepsilon)$ of length $\exp(-O(\varepsilon^{-1}))$ around a critical parameter value $a_c(\varepsilon) = \pm 1 \mp |O(\varepsilon)|$. In particular within this interval the amplitude of the periodic orbit increases by $O(1)$ (uniformly for $\varepsilon \to 0$). The resulting large orbit is a typical example of a relaxation oscillation, featuring fast and slow segments.

Figure 3 shows the phase portraits of orbits $x_a$ for $\varepsilon = 10^{-2}$. The bifurcation diagram plotting the period $T$ versus parameter $a$ in the vicinity of $a_c \approx -0.99874$ is shown in Fig. 4. Most orbits of Fig. 3 lie in the interval $\mathcal{I}_c$ which is of length $\approx \exp(-100)$. Moreover, the orbits stay close to the unstable part of the slow manifold (the light green part of the transparent surface in Fig. 3, which has a $y$-coordinate between $-1$ and $1$) for a time of
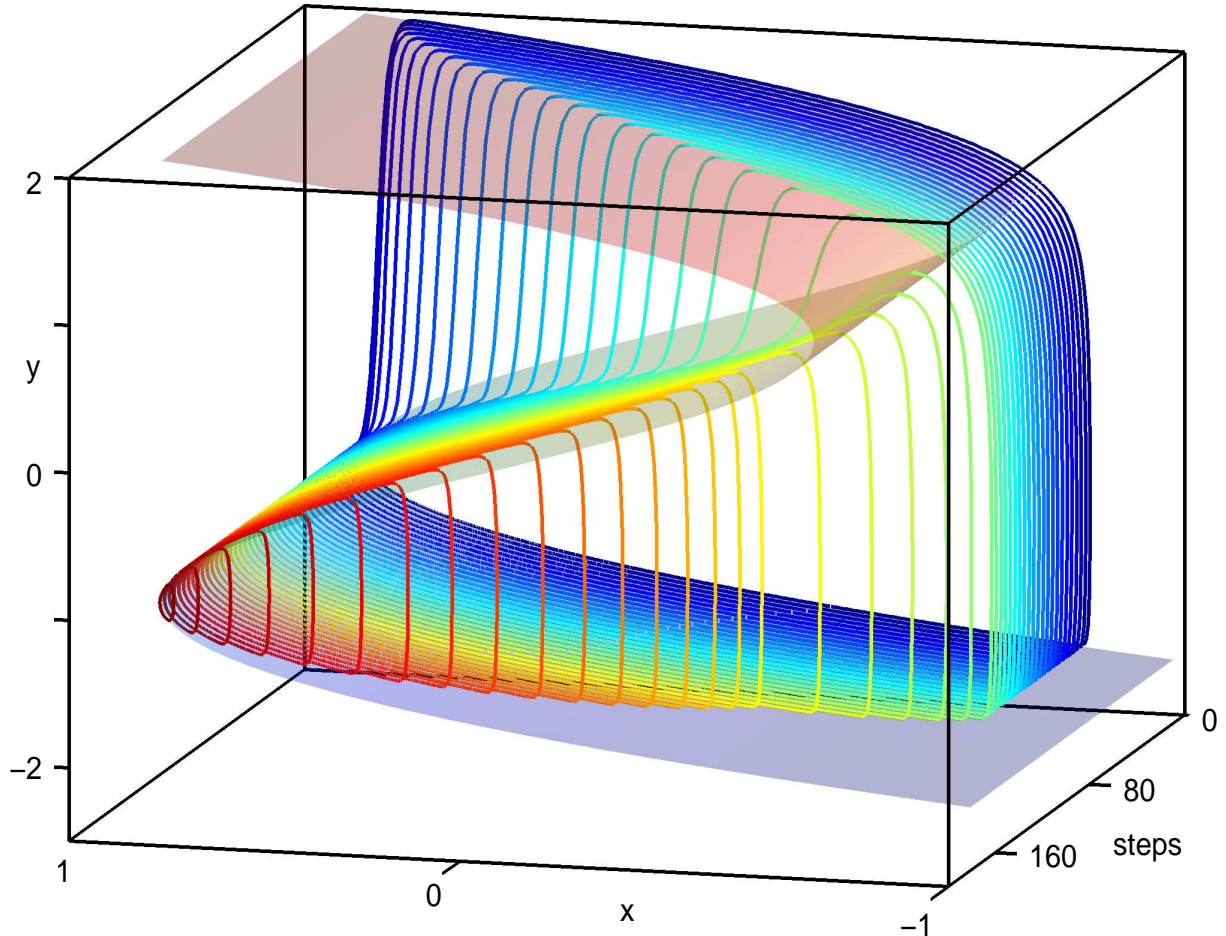
Figure 3: Family of canard periodic orbits in the Van der Pol oscillator with constant forcing (30). The phase portraits are shown in a waterfall plot depending on the step number. The transparent slow manifold visualizes where the canard orbits follow or leave it. The light green part of the slow manifold is transversally unstable. The color coding, which indicates the number of the step along the branch during the continuation, is the same as in Fig. 4.

order $1/\varepsilon$. This makes these orbits extremely sensitive to perturbations. Indeed, a long-time simulation of (30) with numerical error $\gg \exp(-\varepsilon^{-1})$ for $a$ close to $a_c(\varepsilon)$ and small $\varepsilon$ always leaves the unstable part of the slow manifold at a distance of order less than $O(1)$ from the point $(2/3, -1)$. The orbits of $\Gamma$ in the critical interval $\mathcal{I}_c(\varepsilon)$ are called canard periodic orbits due to their counterintuitive following of the slow manifold. The rapid increase of the amplitude is known as a canard explosion. The sensitivity with respect to $a$ and to perturbations makes these canard orbits practically impossible to track in initial value simulations and experiments. Even pseudo-arclength continuation methods that are based on single forward shooting typically fail. On the other hand, continuation methods based on collocation boundary value solvers, such as AUTO (Doedel *et al.* [1998]), are able to compute these orbits reliably. We test the continuation scheme with system (25)–(27) for this example where $a$ is the system parameter $\mu$, $g(x) = I$ and two different values of $k_x$ ($k_x = 5$ and $k_x = 10$; choosing, for example, $g(x) = \begin{bmatrix} 0 & 0 \\ 1 & 1 \end{bmatrix}$ works as well). We note that
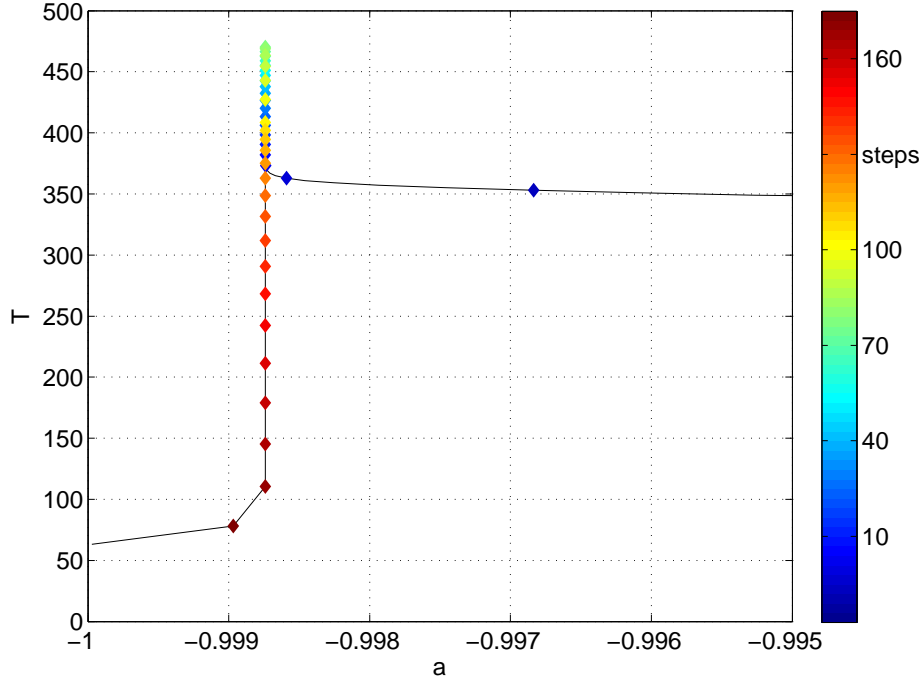
Figure 4: Dependence of the canard orbits on the parameter. The bifurcation diagram show the (extremely sensitive) dependence of the period on the parameter $a$.

these values of $k_x$ are substantially larger than the small gains discussed in Lemma 4. Thus, we cannot expect to be in the range of applicability of Lemma 4 anymore and restrict to the preconditioned system (25)–(27). The coefficient matrix $\partial_1 X$ is computed indirectly via relation (28) and (29) using 12 small deviations $\delta \tilde{x}$.

First, we note that the norm of the inverse of the linearization of the right-hand-side in (25)–(27) is of order less than $k_x/\varepsilon^2$ for $\varepsilon \to 0$ along the canard family. Furthermore, in the controlled problem (24) there is no sensitive dependence of the periodic orbit on $a$ because $k_x \geq 3/4$. This means that the linearization of $X$ is uniformly bounded for $\varepsilon \to 0$ as well. Thus, the problem of continuing periodic orbits using (25)–(27) is well-posed with a Lipschitz constant of order less than $k_x/\varepsilon^2$. Fig. 5 shows the norm of the inverse of the exact linearized right-hand-side (where $X$ has been computed by an explicit integration with $20/\varepsilon$ steps) along the family of canard orbits for two different values of $\varepsilon$ and $k_x$: $\varepsilon = 10^{-1}$, $k_x = 10$ (thick bright blue line); $\varepsilon = 10^{-1}$, $k_x = 5$ (thin dark blue line); $\varepsilon = 10^{-2}$, $k_x = 10$ (thick red line); and $\varepsilon = 10^{-2}$, $k_x = 10$ (thin black line). Note that the $y$-axis has been scaled by the factor $k_x/\varepsilon^2$, which makes curves for the same $\varepsilon$ but different $k_x$ almost identical. The left end corresponds to the large relaxation oscillations and the right end to the Hopf bifurcation. The apparent change in slope near arclength $\approx 0.1$ corresponds to the canard that travels along the complete unstable slow manifold. Figure 5 also gives numerical evidence that the condition of system (25)–(27) increases with proportional to $k_x$. This implies that there is a tradeoff between the efficiency of the evaluation of $X$ (which converges faster to a stable periodic orbit for a large gain $k_x$) and the condition of the problem (25)–(27) defining the periodic orbit.
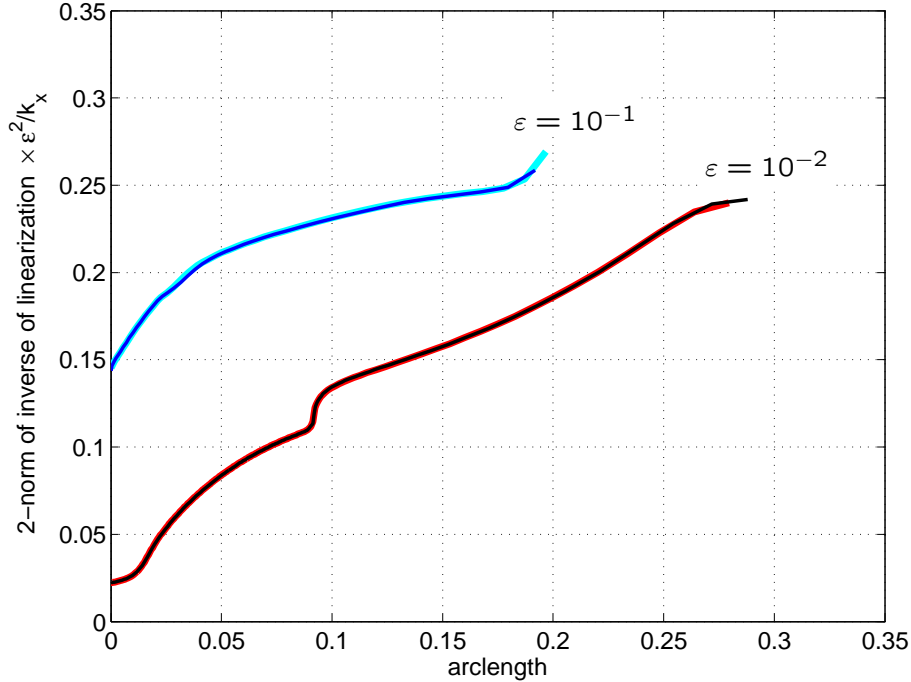
19

Figure 5: $\mathbb{L}^2$ norm of the inverse of the linearized right-hand-side of problem (25)–(27) for the canard family of the Van der Pol oscillator along the branch parameterized by pseudo-arclength for $\varepsilon = 10^{-1}$ (blue and cyan lines) and $\varepsilon = 10^{-2}$ (black and red lines). For each value of $\varepsilon$ there are two curves, one for gain $k_x = 5$ (black and blue (darker) lines) and one for gain $k_x = 10$ (red and cyan (brighter) lines); note that the $y$-axis has been scaled by $k_x/\varepsilon^2$, putting the graphs for different $k_x$ exactly on top of each other so that they are practically indistinguishable.

# 5    Conclusions and Future Work

We introduced a control-based scheme that has potential applications for a pseudo-arclength continuation of periodic orbits in dynamical systems that are run as experiments. The scheme has the advantage that one does not need to evaluate the right-hand-side $f$ of the differential equation directly. Furthermore, in the context of a continuation it is not necessary to set initial values of the state of the dynamical system.

The embedded time-delayed feedback control has the advantage that no approximation of a linearization is necessary. The method converges uniformly near all codimension one bifurcations that border regions of stability. As these bifurcations are of primary interest in many practical applications this method is particularly useful due to its ease of implementation. Of major potential for improving this method are automatic adaptation strategies that do not require an approximation of the full linearization of the problem.

We also proposed the alternative of preconditioning the embedded time-delayed feedback control. The core problem (25)–(27) is well-posed even in cases where other methods that are potentially of use in an experiment (such as methods based on time-1 maps or Poincaré maps) fail. The pointwise evaluation of the right-hand-side of (25) is feasible also in an ex-

periment which allows one to extract a nonlinear equation from measurements. The method does require an approximation of the linearized problem and, as such, is more computationally expensive. Developing more efficient ways to find the linearization under experimental conditions is the subject of ongoing work.

An independent factor that limits the scope of the method is the ability to apply control to the dynamical system in an efficient manner. This factor, which does not play a role in computational simulations, is highly problem-dependent. We believe that hybrid tests are ideal candidates for validating the method presented here, because they inherently allow for greater control. A specific experiment that we are considering is a hybrid test of a parametrically excited pendulum as studied by Kyrychko *et al.* [2005].

# References

Baba, N., Amann, A., Schöll, E., & Just, W. [2002] "Giant improvement of time-delayed feedback control by spatio-temporal filtering," *Phys. Rev. Lett.* **89** (7), 07401.

Bielawski, S., Derozier, D., & Glorieux, P. [1994] "Controlling unstable periodic orbits by a delayed continuous feedback," *Phys. Rev. E* **49** (2), 971–974.

Blakeborough, A., Williams, M., Darby, A., & Williams, D. [2001] "The development of real-time substructure testing," *Philosophical Transactions of the Royal Society of London A* **359**, 1869–1891.

Christini, D., Collins, J., & Linsay, P. [1996] "Experimental control of high-dimensional chaos: The driven double pendulum," *Phys. Rev. E* **54** (5), 4824–4827.

Dhooge, A., Govaerts, W., & Kuznetsov, Y. [2003] "MatCont: a Matlab package for numerical bifurcation analysis of ODEs," *ACM Transactions on Mathematical Software* **29** (2), 141–164.

Doedel, E. J., Champneys, A. R., Fairgrieve, T. F., Kuznetsov, Y. A., Sandstede, B., & Wang, X. [1998] *AUTO97, Continuation and bifurcation software for ordinary differential equations*.

Dumortier, F. & Roussarie, R. [1996] "Canard cycles and center manifolds," *Mem. Amer. Math. Soc.* **121** (577).

Engelborghs, K., Luzyanina, T., & Samaey, G. [2001] "DDE-BIFTOOL v.2.00: a Matlab package for bifurcation analysis of delay differential equations," *Report TW 330, Katholieke Universiteit Leuven*.

Feo, O. D. & Maggio, G. [2003] "Bifurcations in the Colpitts oscillator: from theory to practice," *Int. J. of Bifurcation and Chaos* **13** (10), 2917–2934.

Gauthier, D., Sukow, D., Concannon, H., & Socolar, J. [1994] "Stabilizing unstable periodic orbits in a fast diode resonator using continuous time-delay autosynchronization," *Phys. Rev. E* **50** (3), 2343–2346.

Govaerts, W., Kuznetsov, Y., & Sijnave, B. [2000] "Continuation of codimension-2 equilibrium bifurcations in CONTENT," *Numerical methods for Bifurcation Problems and Large-Scale Dynamical Systems* Doedel E. & L.S.Tuckerman L.S. (Eds.) (Springer-Verlag, New York), pp. 163–184.

Guckenheimer, J., Hoffman, K., & Weckesser, W. [2003] "The forced van der Pol equation I: The slow flow and its bifurcations," *SIAM J. Appl. Dyn. Syst.* **2**, 1–35.

Hale, J. & Lunel, S. V. [1993] *Introduction to Functional Differential Equations* (Springer-Verlag, New York).

Hirsch, M. & Smale, S. [1974] *Differential equations, dynamical systems, and linear algebra.*, vol. 60 of *Pure and Applied Mathematics* (Academic Press, New York–London).

Kevrekidis, I., Gear, C., & Hummer, G. [2004] "Equation-free: The computer-aided analysis of complex multiscale systems," *AIChE Journal* **50** (11), 1346–1355.

Kim, M., Bertram, M., Pollmann, M., von Oertzen, A., Mikhailov, A., Rotermund, H., & Ertl, G. [2001] "Controlling chemical turbulence by global delayed feedback: pattern formation in catalytic CO oxidation on Pt(110)," *Science* **292** (5520), 1357–1360.

Krupa, M. & Szmolyan, P. [2001] "Relaxation oscillations and canard explosion," *J. Differential Equations* **174** (2), 312–368.

Kuznetsov, Y. [2004] *Elements of Applied Bifurcation Theory* (Springer Verlag, New York) Third edition.

Kyrychko, Y., Blyuss, K., Gonzalez-Buelga, A., Hogan, S., & Wagg, D. [2005] Real-time dynamic substructuring in a coupled oscillator-pendulum system," *Proc. Roy. Soc. London A* **462**, 1271–1294.

Nakajima, H. [2004] "Some sufficient conditions for stabilizing periodic orbits without the odd-number property by delayed feedback control in continuous-time systems," *Phys. Lett. A* **327**, 44–54.

Nakajima, H. & Ueda, Y. [1998] "Limitation of generalized delayed feedback control," *Physica D* **111**, 143–150.

Nam, K. & Arapostathis, A. [1992] "A sufficient condition for local controllability of nonlinear systems along closed orbits," *IEEE Transactions on Automatic Control* **37** (3), 378–380.

Pyragas, K. [1992] "Continuous control of chaos by self-controlling feedback," *Phys. Lett. A* **170**, 421–428.

Pyragas, K. [2001] "Control of chaos via an unstable delayed feedback controller," *Phys. Rev. Lett.* **86** (11), 2265–2268.

Siettos, C., Maroudas, D., & Kevrekidis, I. [2004] "Coarse bifurcation diagrams via microscopic simulators: a state-feedback control-based approach," *Int. J. of Bifurcation and Chaos* **14** (1), 207–220.

Socolar, J., Sukow, D., & Gauthier, D. [1994] "Stabilizing unstable periodic orbits in fast dynamical systems," *Phys. Rev. E* **50**, 3245.

Szalai, R., Stépán, G., & Hogan, S. [2004] "Continuation of bifurcations in periodic delay differential equations using characteristic matrices," *SIAM Journal on Scientific Computing* (to appear).

Tronciu, V., Wünsche, H.-J., Radziunas, M., & Wolfrum, M. [2005] Semiconductor laser under resonant feedback from a fabry-perot: stability of continuous wave operation," *Phys. Rev. E* **73** (4), 046205.

Wallace, M., Sieber, J., Neild, S., Wagg, D., & Krauskopf, B. [2005] "Stability analysis of real-time dynamic substructuring using delay differential equation models," *Int. J. of Earthquake Engineering and Structural Dynamics* **34** (15), 1817–1832.

Wieczorek, S., Krauskopf, B., & Lenstra, D. [2000] "Mechanisms for multistability in a semiconductor laser with optical injection," *Optics Communications* **183**, 215–226.

Wieczorek, S., Simpson, T., Krauskopf, B., & Lenstra, D. [2005] "The dynamical complexity of optically injected semiconductor lasers," *Physics Reports* **416**, 1–128.